Materials Research Proceedings 28 (2023) 543-552 https://doi.org/10.21741/9781644902479-59

Investigation of the skin contamination predictability by means of QForm UK extrusion code

KNIAZKIN Ivan[1,a *], PELACCIA Riccardo[2,b], NEGOZIO Marco[3,c], DI DONATO Sara[3,d], DONATI Lorenzo[3,e], REGGIANI Barbara[2,f], BIBA Nikolay [1,g], REZVYKH Ruslan[1,h] and KULAKOV Ivan[1,i]

[1]Micas Simulation Ltd., 107 Oxford Road, Oxford, OX4 2ER, UK

[2]DISMI- Department of Sciences of Methods for Engineering, University of Modena and Reggio Emilia, Viale Amendola 2, 42124, Reggio Emilia, Italy

[3]DIN- Department of Industrial Engineering, University of Bologna, Viale Risorgimento 2, 40136, Bologna, Italy

[a]ivanknjazkin@gmail.com, [b]riccardo.pelaccia@unimore.it, [c]marco.negozio2@unibo.it, [d]sara.didonato2@unibo.it, [e]l.donati@unibo.it, [f]barbara.reggiani@unimore.it, [g]nick@qform3d.com, [h]info@qform3d.com, [i]kulakov@qform3d.com

Keywords: Skin Contamination, Back-End Defect, FEM, QForm Extrusion, ALE Approach

Abstract. The paper presents an innovative approach implemented in QForm UK Extrusion FEM software to analyse one of the core defects encountered in profile extrusion known as billet skin defect. The validation of the algorithm has been performed based on a number of experimental case studies taken from the literature [1,2]. Additionally, the sensitivity of the accuracy of the results to the variation in initial parameters has been analysed for both types of profile shapes: solid and hollow. Based on this, practical recommendations have been formalised for the successful industrial use of the presented algorithm.

Introduction

Aluminium profile extrusion is a process that allows the production of numerous cross-sectional shapes: from simple solid forms to complex hollow shapes. Since these shapes are used for the most highly developed industries, they are subjected to strict requirements regarding geometrical and performance properties. In addition, the modern extrusion process has to be designed to provide high productivity combined with minimal material waste.

One of the typical defects inevitably formed during the direct profile extrusion process is the so-called billet skin defect which is a type of back-end defect. In general, the most critical form of this defect arises during the end of the process cycle if the inlet opening in the tool is incorrectly designed or if the discard length of the billet is too short. Eventually, it causes the penetration of the contaminated content into the profile (Fig. 1).

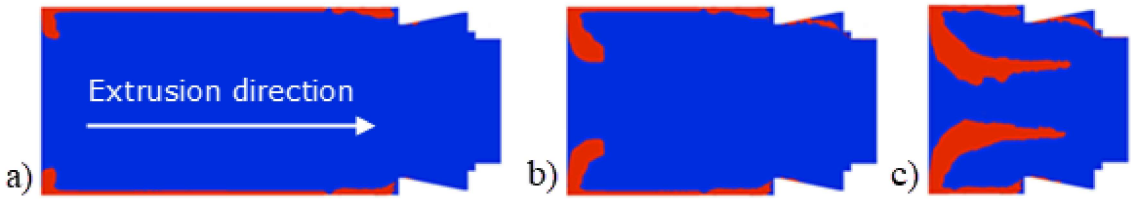

Fig. 1. Stages of extrusion: a) initial, b) intermediate, c) ending. Billet skin is marked by red.

In turn, this results in surface defects and a loss of durability in the finished product [3]. In technical literature it's common to distinguish two types of billet skin flow [2,3]. Flow type 1, also called inward flow, occurs when defective material flows into the tool ports along dead metal zones formed between the container and inlet surface of the tool. Since the material involved in such flow forms the outer shape of the profile, this flow may only lead to surface defects. Whereas, flow type 2, also called forward flow, occurs when the skin layer accumulated at the corner between the container wall and the contact surface of the dummy block starts to flow into the tool ports, causing the appearance of the defective material inside the wall of the profile cross-section.

Skin contamination of the profiles is a potential reason for increasing scrap in the aluminium extrusion process. However, it can be avoided if a proper discard length is chosen to sheer off all the accumulated contaminated material from the skin. The complexity of the process mechanics forcibly invokes the need for a numerical tool to accurately predict the optimal discard length. Even though the impact of the discard length significantly affects the overall process efficiency, few papers have been published on this subject. To the best of authors knowledge, only two studies were performed to investigate the skin defect on profiles of industrial complexity [4,5] where both front-end and back-end defects are analysed using numerical simulation with the Arbitrary Lagrangian Eulerian (ALE) approach. In [6], a Lagrangian approach was used for the simulation of the extrusion process and the skin propagation was checked by tracing the array of points located at the distance of the thickness of contaminated layer. On the one hand, the use of a pure Lagrangian tool resulted in an increase of the prediction accuracy but, on the other hand, it led to a considerable rise in computational time of the simulation.

Unlike the other case studies listed above, this paper aims to find a way to predict the billet skin defect in extruded profile's by means of ALE numerical simulation using an innovative method implemented in QForm UK Extrusion which combines high accuracy in the prediction with low computational time of the simulation.

Description of the Method for Simulation of Billet Skin Propagation

There are two basic ways to describe the motion of deforming material commonly used in numerical simulation, i.e., Lagrangian and Eulerian. Principal differences, limitations and other details of these approaches and their combinations are discussed in [7]. The method used in this paper for billet skin tracking involves points tracing over the Lagrangian-Eulerian mesh environment where points move based on the velocity solution achieved at every step of extrusion simulation of the entire billet.

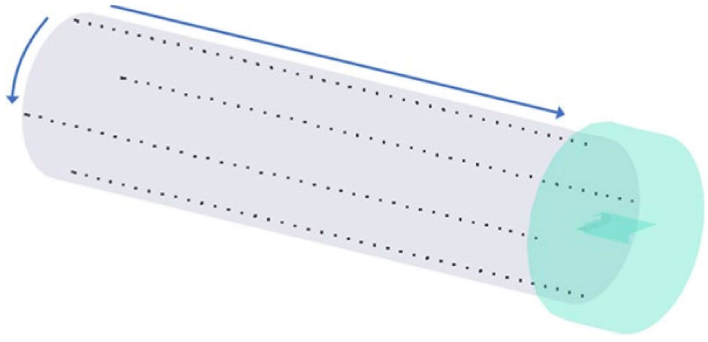

Fig. 2. Initial position of tracking points: 4 lines, 40 points per line.

The settings available as inputs for such kind of analysis are skin thickness, number of lines and number of points per line. Skin thickness value defines the points' radial offset from the upset billet's outer surface. The number of lines is the parameter that determines the number of sectors of the circle so that the points are created along the borders of these sectors. For example, if the number of lines is 2, then there are only two sectors 2x180° with lines located opposite each other,

if the number of lines is 4, then there are four sectors 4x90° (Fig. 2), etc. Additionally, there is a special continuous solid object built based on the specified points. Therefore, there are three different ways to plot the results of such kind of tracing, i.e., array of points, deformed continuous object and billet skin distribution presented in the same way as all the standard typical fields for FEM packages (Fig. 3). This kind of simulation is optional and performed in the post-processor by the implementation of a standard subroutine.

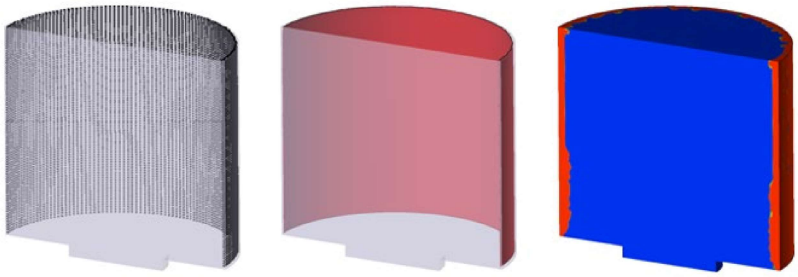

Fig. 3. Types of billet skin representation: array of points (left), continuous solid object (middle), field (right).

Description of the Case Studies

Solid profile.

The authors of the work [1] prepared the special billet with the core material of AA 6063 alloy and skin material of AA 3003 alloy. These materials have similar flow stress levels at high temperatures but react differently to the etching process, therefore billet skin propagation could be clearly recognised on the cross-cuts.

Table 1. Technological and geometrical parameters of the project.

Parameter	Value
Alloy	AA 6063
Extrusion ratio	5.5
Container temperature [°C]	Variable: 20, 500
Billet temperature [°C]	450
Tool temperature [°C]	450
Lubrication	Variable: with and without
Extrusion velocity [mm/s]	19
Billet length [mm]	91
Billet diameter [mm]	91
Container diameter [mm]	94
Ram stroke [mm]	69.5
Billet skin thickness [mm]	1

In this case study, the 40 mm bar was extruded through a flat die under different friction and temperature conditions. There were three experiments carried out, i.e., extrusion without lubricant with a cold container (room temperature), extrusion with a hot container (500°C) without lubrication, and extrusion using a hot container with a lubricated ram. This allowed the authors to obtain different results of metal flow patterns at the contact surfaces between the billet and tools, which eventually affected the shape of the contaminated layer. Process parameters and geometrical detail are listed in Table 1.

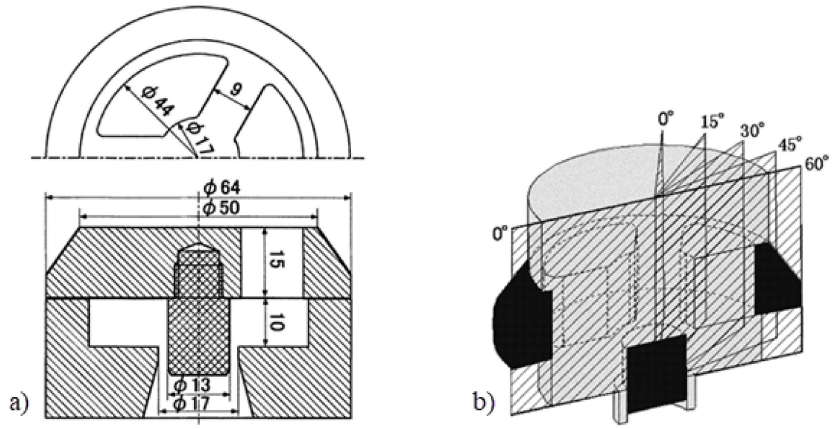

Fig. 4. Geometrical details of the second case study: a) tool scheme; b) cross-cut planes analysed in experiment (right).

Hollow profile.

In this case [2], AA 1100 alloy was used as a core material and AA 1050 as a billet skin material. Similar to the first presented case, the etching characteristics of the alloys differed, allowing qualitative identification of the billet skin propagation. For this purpose, the authors have designed a porthole tool with sixfold symmetry (Fig. 4a). The investigation was divided into two significant steps: analysis of the evolution of billet skin shape at different ram strokes for the case where no lubrication was used, and analysis of billet skin pattern depending on different friction conditions on ram and container. For both cases, the results of billet skin propagation were analysed for five different planes (Fig. 4b). Technological parameters and critical dimensions of the project are listed in Table 2. The authors of the work also performed tests using colloidal graphite lubrication but this part of the experiment isn't considered in the current paper.

According to the presented data, several simulations were done using a coupled thermomechanical task for the material flow domain and tools (Fig. 5).

Table 2. Technological and geometrical parameters of the project.

Parameter	**Value**
Alloy	AA 1100
Extrusion ratio	20.9
Container temperature [°C]	400
Billet temperature [°C]	400
Die temperature [°C]	400
Lubrication	Variable: no lubricant, boron nitride
Extrusion velocity [mm/s]	0.017
Billet length [mm]	50
Billet diameter [mm]	49.5
Container diameter [mm]	50
Ram stroke	Variable: from 35 to 46
Billet skin thickness [mm]	0.5

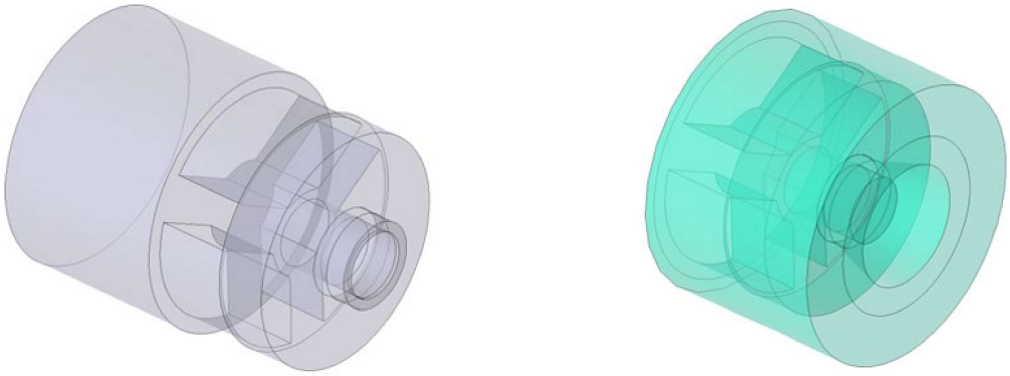

Fig. 5. Geometrical representation of the second case study: material flow domain (left) and porthole tool (right).

Description of the Models Used in the Simulation

Coupled task.

Material flow and temperature are simulated, taking into account the deformation of the tool and the temperature distribution in it. This means that tool deformation influences the material flow, while the tool distortion itself depends on the material's contact pressure. Similarly, temperature evolution in billet material is defined not only by heat generation due to plastic deformation and friction but also by heat exchange with the tool. Such a coupled solution is obtained through several iterations combined with automated remeshing of the flow domain. The heat flux between the billet and tooling set is specified by Newton-Richmann law in the following form:

$$q_n = \alpha(T_1 - T_2) \tag{1}$$

where α - heat transfer coefficient (by default equal to 30000 W/m^2K in QForm UK Extrusion), which takes into account the number of coefficients of heat transfer between the workpiece and lubrication and between lubrication and the tool, T_1 is the billet temperature, T_2 is the tool temperature.

Table 3. Hensel-Spittel parameters for AA 6063 and AA 1100.

Parameter	Solid design	Hollow design
A [MPa]	250.7	265
m_1 [K^{-1}]	-0.000498	-0.00458
m_2	0.126346	-0.12712
m_3	0.135122	0.12
m_4	-0.0052884	-0.0161
m_5 [K^{-1}]	-1.06775x10^{-6}	0.00026
m_7	0.00005655	0
m_8 [K^{-1}]	2.53717 x10^{-8}	0
m_9	0	0

Flow stress.

Hensel-Spittel equation (2) defines the dependence of the flow stress (σ_s) on the strain (ε), strain-rate ($\dot{\varepsilon}$), and temperature ($\boldsymbol{T}$) were used to describe flow curves for the billet material used in both considered projects. Table 3 contains values of the coefficients used in the simulation.

$$\sigma_s = A \cdot e^{m_1 T} \cdot T^{m_9} \cdot \varepsilon^{m_2} \cdot e^{\frac{m_4}{\varepsilon}} \cdot (1+\varepsilon)^{m_5 T} \cdot \varepsilon^{m_7 \varepsilon} \cdot \dot{\varepsilon}^{m_3} \cdot \dot{\varepsilon}^{m_8 T} \quad (2)$$

Friction.

Levanov friction law was used to describe friction between aluminium and steel. This friction model is a generalisation of the Coulomb and Siebel friction laws. When the normal contact pressure is low (typical for the bearing area), Levanov's shear stress is close to Coulomb's. When the normal contact pressure is high (which is typical for the rest of the billet usrface), Levanov's shear stress is close to Siebel's shear stress. According to the Levanov friction model, the shear stress (τ) on the contacting surface of the workpiece depends on the friction factor ($\boldsymbol{m}$), flow stress ($\sigma_{\boldsymbol{s}}$) of the workpiece material, normal contact pressure ($\sigma_{\boldsymbol{n}}$), and Levanov coefficient ($\boldsymbol{n}$):

$$\tau = m \cdot \frac{\sigma_s}{\sqrt{3}} \cdot \left(1 - e^{-n \cdot \frac{\sigma_n}{\sigma_s}}\right) \quad (3)$$

In QForm UK Extrusion the default value of Levanov coefficient that was used for all simulations is equal to 1.25.

Mesh.

To investigate the impact of initial mesh size, two different mesh variations were created for both hollow and solid profile designs, where an increased adaptation coefficient in the container area was used to make the mesh finer. The visual and quantitative differences between the initial and adapted mesh can be seen in Fig. 6 and Table 4, respectively.

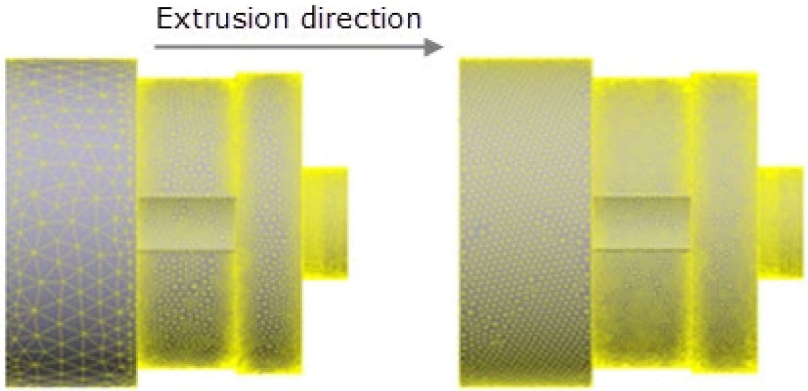

Fig. 6. Initial (left) and adapted (right) mesh for hollow profile.

It's been observed that for the proposed approach mesh density influenced the smoothness of the resulting skin shape but didn't significantly affect the qualitative picture of its propagation. Therefore, further analysis is presented for the cases with mesh generated with the default settings.

Table 4. Mesh properties.

	Initial mesh	**Adapted mesh**
Nodes, #	145586	174961
Surface elements, #	70958	91570
Volume elements, #	786554	931870

Materials Research Proceedings 28 (2023) 543-552 https://doi.org/10.21741/9781644902479-59

Results and Discussion

Solid profile.

The simulation of the extrusion process was performed using standard hot AA 1100 alloy available in the QForm material database. The total computational time for the simulation resulted in 2 hours. For the cases where no lubrication was used in actual experiments, the friction properties were selected according to the default extrusion settings, i.e., Levanov friction law with the friction factor equal to 1. For the experiment where lubrication was used, the friction factor (m) was assumed to be equal to 0.5 in simulation to evaluate the sensitivity of this parameter on the final result.

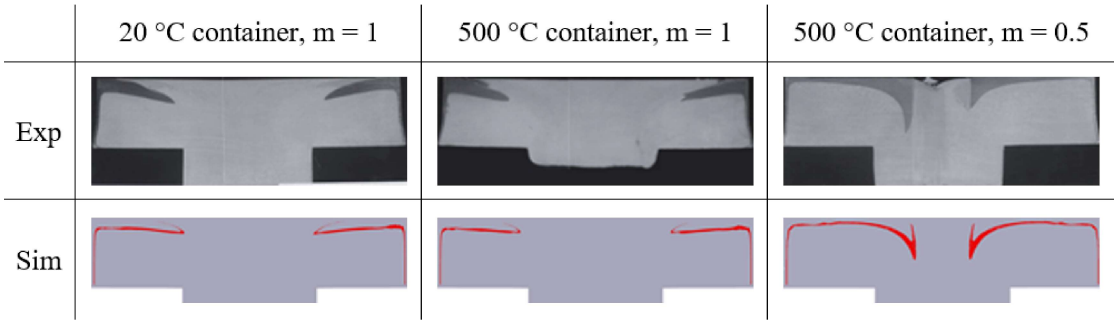

Fig. 7. Comparison of billet skin propagation in experiments with the solid profile.

As it can be clearly seen from Fig. 7, simulation has fully matched the experimental results. It's worth mentioning that the difference in container temperature (20°C vs 500°C) had no significant effect on the results of billet skin flow. Which is quite logical in this case since the design configuration is simple and difference in temperature doesn't affect the general behaviour of the flow pattern.

Nevertheless, the change in friction conditions on the ram surface led to a significant change in the billet skin shape. In this case, the use of lubricant worsened the flow pattern of billet skin since the contaminated material is located closer to the bearing exit of the tool.

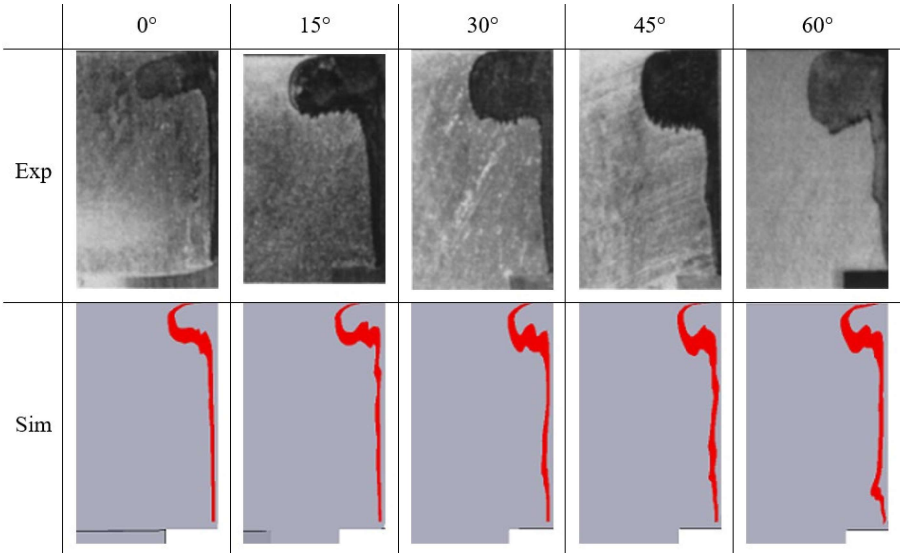

Fig. 8. Comparison of billet skin propagation in the experiment without lubrication and simulation for 35 mm ram stroke.

It can also be seen that the experimental result in the case of the lubricated contact surface of the ram is remarkably asymmetrical. It could be caused by different production factors such as inaccurate container alignment, an asymmetrical upsetting of the billet in the container, etc. In a simulation the asymmetry is also possible but mostly due to the difference in the mesh. In general, such kind of asymmetry can be minimised or even eliminated by making the mesh finer or by the use of symmetry planes.

Hollow profile.

In this case, the simulation was performed with standard extrusion AA 6063 alloy from the QForm material database. The total computational time for the simulation resulted in 3 hours and 30 minutes. As mentioned before, the first step of algorithm verification was to assess the evolution of billet skin shape at different ram strokes. For all the experiments where no lubrication was used, the friction conditions were set in accordance with the default extrusion friction available in the QForm database mentioned before.

Fig. 8 presents the results of the first test where the process was stopped at 35 mm ram stroke. It can be seen that the most intensive propagation of the contaminated layer is achieved on the cross-cut located in the middle of the port (60°). The area of billet skin decreases as you move away from this section reaching its minimum on the cross-cut plane (0°) placed right in the middle of the mandrel web (separation element of the tool). Simulation shows a similar trend of billet skin propagation qualitatively matching experimental results. For both practical and simulation results the origination of inward flow can be seen in sections 45° and 60°.

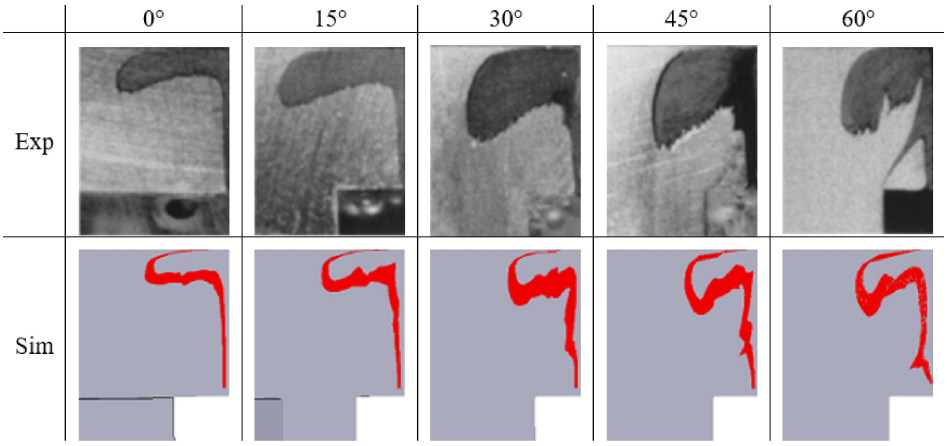

Fig. 9. Comparison of billet skin propagation in the experiment without lubrication and simulation for 41 mm ram stroke.

Fig. 9 compares the results of the same test but with the ram stroke equal to 41 mm. In this case, the inward flow is clearly defined for section 60°, which determines the intensive metal flow from the regions close to the container surface. Whereas the flow in section 0° that crosses the middle of the web has no sign of inward flow and billet skin propagates radially along the ram surface. For this stage of the process (41 mm ram stroke) simulation shows qualitatively the same result obtained in the practical experiment, which indirectly confirms the general correctness of the initial parameters used in the simulation. Slight deviations in inward flow might be caused by the sensitivity of this kind of back-end defect to the mesh size, specifics of the tracing algorithm or billet skin visualisation in the software.

In a similar way, Fig. 10 presents the results of the final moment of the extrusion process of the billet for the ram stroke equal to 46 mm. At this stage contaminated material flows into the ports for the sections 30°, 45° and 60°.

Materials Research Proceedings 28 (2023) 543-552 https://doi.org/10.21741/9781644902479-59

Another part of the investigation in this experiment was assessing the impact of lubrication on the flow pattern of billet skin. To simulate this influence, the friction factor was assumed to be equal to 0.9 on the contact surfaces of the ram and container. In this case, simulation matched the experimental result quite well (Fig. 11) with a minor deviation that adjustment of the friction factor

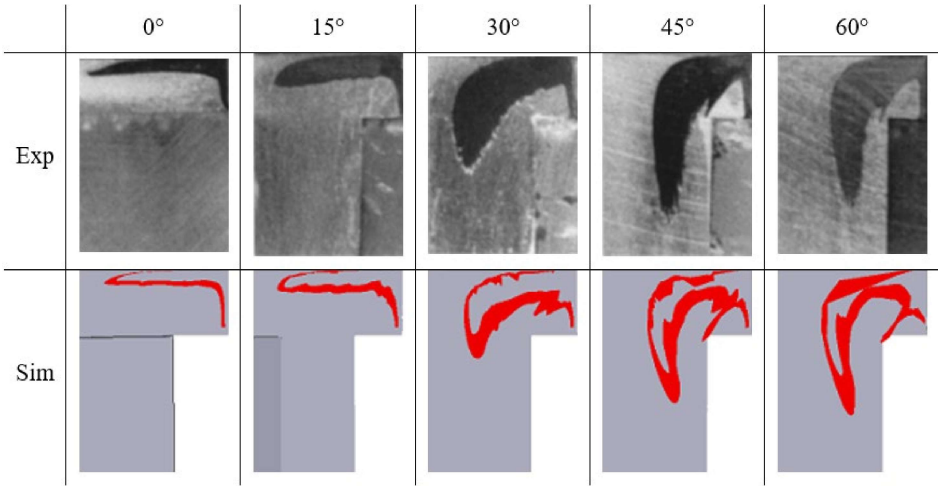

Fig. 10. Comparison of billet skin propagation in experiment without lubrication and simulation for 46 mm ram stroke.

can eliminate. In this case, if compared with the process that was carried out without lubrication for a similar ram stroke, it can be clearly seen that the volume of contaminated material approaching the ports is less, which indicates the positive influence of lubrication on billet skin propagation in contrast to the result obtained for the solid profile. However, it should be noted that containers of direct extrusion of aluminium profiles are generally not lubricated in industrial conditions.

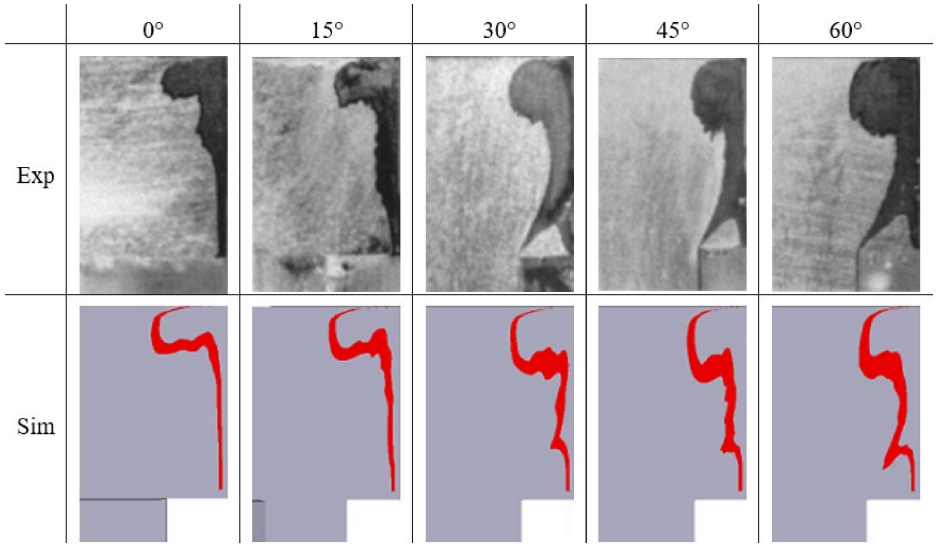

Fig. 11. Comparison of billet skin propagation in experiment with BN lubrication and simulation for 39 mm ram stroke.

Summary

In the present work, the innovative method of billet skin prediction implemented in QForm UK Extrusion was used and verified based on two experimental studies. It's worth noting that from a practical point of view, the results obtained in cases where no lubrication was used have a higher

value, since most industrial extrusion trials are performed without any lubrication of the container, ensuring the adhesion of billet aluminium to tool steel. The qualitative comparison was carried out for solid and hollow profiles extruded with different friction conditions. Parameters affecting the accuracy of this method have been varied to define the sensitivity of the applied approach.

As a summary, the presented research allows us to draw the following key findings:

- A good numerical-experimental matching was achieved on the skin contamination behaviour with and without lubrication.
- The total computational time for the two simulations (2 hours for the solid profile, 3 hours, and 30 min for the hollow profile) proved to be several times lower than the computational time reported in [6] without causing a decrease in the prediction accuracy. PC with Intel Core i9-9940X (14 cores, 4.20 GHz max. frequency) was used to obtain simulation results.
- Friction is a crucial parameter affecting the propagation of the contaminated layer.
- Default friction settings recommended for simulation in QForm UK Extrusion provided high accuracy of the results for experiments carried out without lubrication.
- Lubrication can lead to both positive and negative effects on the propagation of the contaminated layer.
- Even a significant change in container temperature has a minor effect on the flow pattern of billet skin in case of extrusion of simple solid bars.

References

[1] Y.T. Kim, K. Ikeda, Flow behaviour of the billet surface layer in porthole die extrusion of aluminum, Metall. Mater. Trans. A 31 (2000) 1635-1643. https://doi.org/10.1007/s11661-000-0173-4

[2] T. Ishikawa, H. Sano, Y. Yoshida, N. Yukawa, J. Sakamoto, Y. Tozawa, Effect of Extrusion Conditions on Metal Flow and Microstructures of Aluminum Alloys. CIRP Annals 55(1) (2006) 275-278. https://doi.org/10.1016/S0007-8506(07)60415-6

[3] H.S. Valberg, M. Lefstad, A.L. de Moraes Costa, On the mechanism of formation of back-end defects in the extrusion process, Procedia Manuf. 47 (2020) 245-252. https://doi.org/10.1016/j.promfg.2020.04.207

[4] S. Lou, Y. Wang, C. Liu, S. Lu, C. Su, Analysis and Prediction of the Billet Butt and Transverse Weld in the Continuous Extrusion Process of a Hollow Aluminum Profile, J. Mater. Eng. Perform. 26 (2017) 4121- 4130. https://doi.org/10.1007/s11665-017-2771-y

[5] M. Negozio, R. Pelaccia, L. Donati, B. Reggiani, L. Tomesani, T. Pinter, FEM Validation of front end and back end defects evolution in AA6063 and AA6082 aluminum alloys profiles, Procedia Manuf. 47 (2020) 202-208. https://doi.org/10.1016/j.promfg.2020.04.178

[6] M. Negozio, R. Pelaccia, L. Donati, B. Reggiani, FEM Analysis of the Skin Contamination Behavior in the Extrusion of a AA6082 Profile, Key Eng. Mater. 926 (2022) 452-459. https://doi.org/10.4028/p-y37nm3

[7] I. Kniazkin, Prediction of Underfilling Defect in Aluminium Profile Extrusion Based on ALE Simulation, Key Eng. Mater. 926 (2022) 537-544. https://doi.org/10.4028/p-42gaq6